

N-Methyl-D-Aspartate Receptor-Driven Calcium Influx Potentiates the Adverse Effects of Myocardial Ischemia-Reperfusion Injury Ex Vivo

Zi-You Liu, PhD, Shou Hu, MD, Qin-Wen Zhong, MD, Cheng-Nan Tian, MD, Hou-Mou Ma, MD, and Jun-Jian Yu, MD

Background: Despite the adverse effects of N-methyl-D-aspartate receptor (NMDAR) activity in cardiomyocytes, no study has yet examined the effects of NMDAR activity under ex vivo ischemic-reperfusion (I/R) conditions. Therefore, our aim was to comprehensively evaluate the effects of NMDAR activity through an ex vivo myocardial I/R rat model.

Methods: Isolated rat hearts were randomly segregated into 6 groups ($n = 20$ in each group): (1) an untreated control group; (2) a NMDA-treated control group; (3) an untreated I/R group; (4) an I/R+NMDA group treated with NMDA; (5) an I/R+NMDA+MK-801 group treated with NMDA and the NMDAR inhibitor MK-801; and (6) an I/R+NMDA+[Ca²⁺]_i-free group treated with NMDA and [Ca²⁺]_i-free buffer. The 4 I/R groups underwent 30 minutes of ischemia followed by 50 minutes of reperfusion. Left ventricular pressure signals were analyzed to assess cardiac performance. Myocardial intracellular calcium levels ([Ca²⁺]_i) were assessed in isolated ventricular cardiomyocytes. Creatine kinase, creatine kinase isoenzyme MB, lactate dehydrogenase, cardiac troponin I, and cardiac troponin T were assayed from coronary effluents. TTC and TUNEL staining were used to measure generalized myocardial necrosis and apoptosis levels, respectively. Western blotting was applied to assess the phosphorylation of PKC- δ , PKC- ϵ , Akt, and extracellular signal-regulated kinase.

Results: Enhanced NMDAR activity under control conditions had no significant effects on the foregoing variables. In contrast, enhanced NMDAR activity under I/R conditions produced significant increases in [Ca²⁺]_i levels (~1.2% increase), significant losses

in left ventricular function (~5.4% decrease), significant multi-fold increases in creatine kinase, creatine kinase isoenzyme MB, lactate dehydrogenase, cardiac troponin I, and cardiac troponin T, significant increases in generalized myocardial necrosis (~36% increase) and apoptosis (~150% increase), and significant multi-fold increases in PKC- δ , PKC- ϵ , Akt, and extracellular signal-regulated kinase phosphorylation (all $P < 0.05$). These adverse effects were rescued by the NMDAR inhibitor MK-801 or [Ca²⁺]_i-free buffer (all $P < 0.05$).

Conclusions: NMDAR-driven calcium influx potentiates the adverse effects of myocardial I/R injury ex vivo.

Key Words: N-methyl-D-aspartate receptor, NMDAR, NMDA, cardiac, cardiomyocyte, myocardial, ischemic-reperfusion, I/R

(*J Cardiovasc Pharmacol*TM 2017;70:329–338)

INTRODUCTION

The N-methyl-D-aspartate receptor (NMDAR) is an ionotropic glutamate receptor that primarily functions as a calcium ion transporter.¹ Although previous NMDAR research has focused on its role in neuropsychiatric dysfunction,^{2,3} the NMDAR has also been shown to play a key role in cerebral ischemia.^{4,5} Specifically, NMDAR activity has been shown to drive the neurotoxic calcium influx observed with cerebral ischemia.⁶ Accordingly, several NMDAR blockers (eg, Cerestat, traxoprodil, remacemide, selfotel, and licostinel) have demonstrated promising neuroprotective effects in animal models of cerebral ischemia.⁷

Although NMDAR research has been primarily associated with the central nervous system, Gill et al.'s group has demonstrated that NMDAR is expressed in cardiomyocytes as well.^{8,9} This discovery has led to a speculation that NMDAR may play a role in myocardial ischemia.¹⁰ Although NMDAR activity has not been directly associated with myocardial ischemia, NMDAR activation has been shown to promote mitochondrial calcium influx and increased oxidative stress in rat cardiomyocytes—an effect that is abolished by NMDAR blockade.¹¹ Moreover, myocardial ischemic preconditioning has been shown to induce calcium influx and to activate downstream signaling intermediaries previously associated with CNS-expressed NMDAR, such as protein kinase C (PKC) and the mitogen-activated protein kinase extracellular signal-regulated kinase (ERK).^{10,12,13} In addition, recent work by our research group has shown that NMDAR antagonism by MK-801 rescues the adverse effects

Received for publication September 10, 2016; accepted May 18, 2017.

From the Department of Heart Center, The First Affiliated Hospital of Gannan Medical University, Ganzhou, Jianxi, China.

Supported by the National Natural Science Foundation of China (grant no. 81360287) and the Science Foundation of Jianxi Education (grant no. GJJ12547).

The authors report no conflicts of interest.

Z.-Y. Liu and H.-M. Ma: conceived and designed the study. Q.-W. Zhong, C.-N. Tian, and H.-M. Ma: performed the experiments. J.-J. Yu and S. Hu: analyzed the data. Z.-Y. Liu: drafted the manuscript.

Reprints: Zi-You Liu, The Heart Center, The First Affiliated Hospital of Gannan Medical University, No. 23 Qinnian Rd, Ganzhou, Jianxi 341000, China (e-mail: gzziyoudoc@126.com).

Copyright © 2017 The Author(s). Published by Wolters Kluwer Health, Inc. This is an open-access article distributed under the terms of the Creative Commons Attribution-Non Commercial-No Derivatives License 4.0 (CCBY-NC-ND), where it is permissible to download and share the work provided it is properly cited. The work cannot be changed in any way or used commercially without permission from the journal.

of NMDAR-driven calcium influx in an in vitro OGD cardiomyocyte model (unpublished data).

Despite this previous evidence supporting the adverse effects of NMDAR activity in cardiomyocytes, no study has yet examined the effects of NMDAR activity under myocardial ischemic-reperfusion (I/R) conditions. We hypothesized that NMDAR-driven calcium influx potentiates the adverse effects of myocardial I/R injury. Therefore, the aim of this study was to comprehensively evaluate the effects of NMDAR activity through an ex vivo myocardial I/R rat model.

MATERIALS AND METHODS

Ethics Statement

This study was conducted according to the National Institutes of Health (NIH) Guide for the Care and Use of Laboratory Animals.¹⁴ The study protocols involving animal subjects were approved in advance by the Animal Ethics Committee of the Gannan Medical University (approval no. 201233). All efforts were made to minimize animal suffering.

Preparation of Isolated Rat Hearts

Isolated rat hearts were prepared as previously described by Hu et al with minor modifications.¹⁵ One hundred adult male Sprague-Dawley rats (weight range: 200–250 g) were first injected with sodium pentobarbital (50 mg/kg intraperitoneally) followed by injection with heparin (50 IU intravenously). Then, the rat hearts were rapidly dissected out of their thoracic cavities and gently put in ice-cold (4°C) Krebs–Henseleit buffer solution (118 mM NaCl, 25 mM NaHCO₃, 11 mM glucose, 4.7 mM KCl, 1.25 mM CaCl₂, 1.2 mM KH₂PO₄, and 1.2 mM MgSO₄; pH 7.4). The rat hearts were then positioned on a Langendorff instrument for perfusion as described below.

Construction of Ex Vivo Global Myocardial I/R Model

The isolated rat hearts were randomly segregated into 6 groups (n = 20 in each group): (1) an untreated healthy control group (the control group); (2) a NMDA-treated control group (the NMDA group); (3) an untreated I/R group (the I/R

group); (4) an NMDA-treated I/R group (the I/R+NMDA group); (5) a NMDA-treated and MK-801-treated I/R group (the I/R+NMDA+MK-801 group), and (6) a [Ca²⁺]-free, NMDA-treated I/R group (the I/R+NMDA+[Ca²⁺]-free group) (Fig. 1). The isolated rat hearts underwent baseline equilibration with gas-infused Krebs–Henseleit buffer (95% O₂, 5% CO₂) at 80 mm Hg pressure for a 20-minute period (37°C). Then, the isolated rat hearts were treated according to their respective grouping for a period of 10 minutes as follows (all 37°C): (1) the control group was left untreated on the gas-infused Krebs–Henseleit buffer; (2) the NMDA group was treated with 0.1 mM NMDA in the gas-infused Krebs–Henseleit buffer; (3) the I/R group was left untreated on the gas-infused Krebs–Henseleit buffer; (4) the I/R+NMDA group was treated with 0.1 mM NMDA in the gas-infused Krebs–Henseleit buffer; (5) the I/R+NMDA+MK-801 was treated with 0.1 mM NMDA and 30 μM MK-801 in the gas-infused Krebs–Henseleit buffer; and (6) the I/R+NMDA+[Ca²⁺]-free group was treated with 0.1 mM NMDA and [Ca²⁺]-free, gas-infused Krebs–Henseleit buffer solution. The dosages of 0.1 mM NMDA and 30 μM MK-801 applied here are based on previous research in neonatal rat cardiomyocytes by Gao et al¹¹

After the 10-minute treatment period, the rat hearts in the 4 I/R groups (ie, the I/R group, I/R+NMDA group, I/R+NMDA+MK-801, and the I/R+NMDA+[Ca²⁺]-free group) underwent global myocardial I/R by ceasing the Krebs–Henseleit perfusion for 30 minutes (ischemia) immediately followed by reperfusion for 50 minutes (37°C), as previously described by Hu et al¹⁵ Reperfusion was performed using the same solutions applied during the 10-minute treatment period (see above). The control groups were not subjected to I/R and were left on the gas-infused Krebs–Henseleit buffer.

Ventricular Pressure Measurement

As previously described by Hu et al,¹⁵ saline-fillable latex balloon was threaded through the left atrial chamber and the mitral valve into the left ventricular chamber. Then, the balloon was inflated to reach a left ventricular end-diastolic pressure (LVEDP) of less than 10 mm Hg. The left ventricular developed pressure (LVDP) as well as the maximal rates of LVDP gains (+dP/dt) and losses (–dP/dt) were measured through a MP150 pressure transducer (BIOPAC

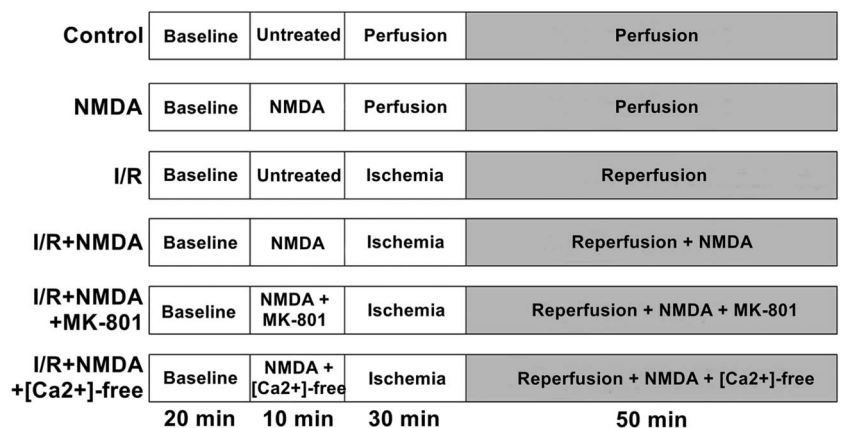


FIGURE 1. Experimental overview: 6 groups (n = 20 each) were constructed to assess the effects of NMDAR-driven influx: (1) a control group, (2) a NMDA group, (3) an I/R group; (4) an I/R+NMDA group; (5) an I/R+NMDA+MK-801 group, and (6) an I/R+NMDA+[Ca²⁺]-free group.

Systems, Santa Barbara, CA) attached to the balloon. LVDP was calculated as the difference between left ventricular end-systolic pressure (LVESP) and LVEDP (ie, $LVDP = LVESP - LVEDP$). Left ventricular pressure signals were recorded and analyzed using AcqKnowledge 3.8.1 package (BIOPAC Systems).

Measurement of Myocardial Intracellular Calcium Levels ($[Ca^{2+}]_i$)

Ventricular cardiomyocytes were isolated from the rat hearts using Saini et al.'s method.¹⁶ Then, the isolated ventricular cardiomyocytes were treated in a fura-2 AM buffer (5 μ M fura-2 AM with 1 mM Ca^{2+} , pH 7.4) for 40 minutes. The cells were then rinsed twice to remove excess dye. For standardization, the cell density within the cuvette was set to 300,000 cells/mL per experimental group. Fluorescent intensities were measured with a dual-wavelength spectrofluorometer (RF-5000, Shimadzu Corporation, Kyoto, Japan) using the following parameters: 340/380-nm excitation wavelength, 510-nm emission wavelength, 0.95-s integration time, and 1.0-s resolution time. $[Ca^{2+}]_i$ levels were assessed with the Grynkiewicz formula as follows¹⁷: $[Ca^{2+}]_i = K_d \times [(R - R_{min}) / (R_{max} - R) \times Sf_2 / Sb_2]$, where R is the fluorescence signal ratio derived from 340-nm and 380-nm excitation wavelengths, R_{max} and R_{min} are the R values after adding 10% Triton X-100 (20 μ L) and 400 mM EGTA (40 μ L), respectively, and Sf_2 and Sb_2 are the fluorescence proportionality coefficients (measured at a 380-nm excitation wavelength) obtained under R_{min} and R_{max} conditions, respectively.

Cardiac Marker Assays

Creatine kinase (CK), creatine kinase isoenzyme MB (CK-MB), lactate dehydrogenase (LDH), cardiac troponin I (cTnI), and cardiac troponin T (cTnT) levels were assayed as previously described by Hu et al with minor modifications.¹⁵ Coronary effluents were collected immediately after the 20-minute baseline equilibration period and immediately after the 50-minute reperfusion period. Activity levels for all 5 cardiac markers were assayed spectrophotometrically using their respective kits according to the kits' instructions (Jiancheng Reagent Co, Nanjing, China). Activity levels of all 5 cardiac markers were calculated using their respective standard curves.

Assessment of Generalized Myocardial Necrosis

As previously described by Hu et al,¹⁵ staining with 2,3,5-triphenyltetrazolium chloride (TTC; Sigma Chemical, St. Louis, MO) was used to measure generalized myocardial necrosis. Immediately after the aforementioned 50-minute reperfusion period, the rat hearts were frozen to $-20^\circ C$ for 3 hours. The resulting frozen ventricular tissue was sliced into sections (2–3 mm) and then incubated in 1% TTC dissolved in 0.1 M Tris buffer (pH 7.8) at $37^\circ C$ for 15 minutes. Slices were captured by digital photography followed by imaging analysis with Image 1.38 (NIH, Bethesda, MD). Generalized myocardial necrosis was measured as the proportion of the sectioned area.

Apoptosis Assay

As previously described by Hu et al,¹⁵ the one step terminal deoxynucleotidyl transferase dUTP nick end labeling (TUNEL) apoptosis assay kit (Beyotime Biotechnology, Haimen, Jiangsu, China) was used to assay apoptosis levels in the ventricular tissue sections. A TUNEL stain (green fluorescent dye; Beyotime Biotechnology) was applied to identify apoptotic cells, whereas 6-diamino-2-phenylindole (DAPI) stain (blue fluorescent dye; Beyotime Biotechnology) was applied to identify all cardiomyocytes. Fluorescence microscopy (Olympus IX81, Tokyo, Japan) was used to perform cellular counts. Ten visual fields were randomly chosen for each sample.

Western Blotting of Protein Kinases

As previously described by Hu et al,¹⁵ total protein (30 mg from each sample) was separated by sodium dodecyl sulfate polyacrylamide gel electrophoresis with 8% acrylamide gels used for total PKC- δ , p-PKC- δ (Ser⁶⁴³), total PKC- ϵ , and p-PKC- ϵ (Ser⁷²⁹), and 10% acrylamide gel was used for total Akt, p-Akt(Ser⁴⁷³), p-Akt(Thr³⁰⁸), total ERK, and p-ERK(Thr⁴⁰²-Tyr²⁰⁴). After transfer onto polyvinylidene difluoride membranes, the membranes were then subjected to overnight incubation at $4^\circ C$ with the following primary antibodies (diluted 1:1000 in blocking buffer; Cell Signaling Technology (Danvers, MA) unless otherwise noted): anti-PKC- δ , anti-p-PKC- δ (Ser⁶⁴³), anti-PKC- ϵ , anti-p-PKC- ϵ (Ser⁷²⁹) (Upstate), anti-Akt, anti-p-Akt(Ser⁴⁷³), anti-p-Akt(Thr³⁰⁸), anti-ERK, anti-p-ERK(Thr⁴⁰²-Tyr²⁰⁴), and anti- β -actin (Sigma, loading control). Following a 15-minute rinsing with Tris-buffered saline+Tween 20, the polyvinylidene difluoride membranes were then treated with horseradish peroxidase-conjugated secondary antibodies. The resulting bands were identified by ECL followed by analysis with Quantity One 4.5 package (Bio-Rad, Hercules, CA).

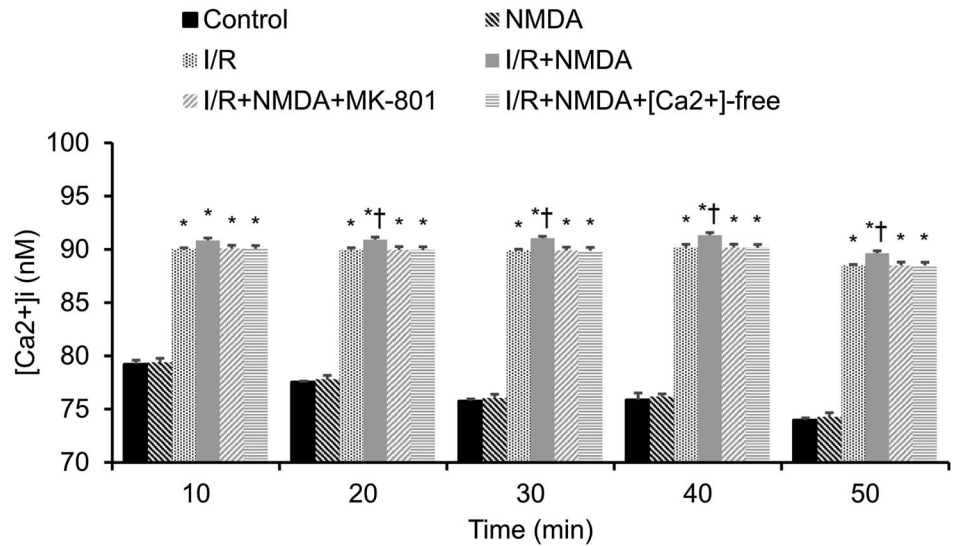
Statistical Analysis

Results were expressed as mean and associated standard errors of the mean (SEMs). Comparisons between 2 groups were conducted by Student's *t*-testing, whereas comparisons between more than 2 groups were conducted by 2-way analysis of variance. A *P* value of < 0.05 was deemed significant.

RESULTS

We first assessed myocardial intracellular calcium levels ($[Ca^{2+}]_i$) over the 50-minute reperfusion period to examine the effect of NMDAR activity on myocardial calcium influx. NMDA treatment under control conditions had no significant effect on $[Ca^{2+}]_i$ ($P > 0.05$, Fig. 2). After global myocardial I/R, there was a significant elevation in $[Ca^{2+}]_i$ relative to control conditions ($\sim 17\%$ increase, $P < 0.05$, Fig. 2). Notably, treatment with NMDA under I/R conditions produced a slightly more pronounced elevation in $[Ca^{2+}]_i$ at the 20-, 30-, 40-, and 50-minute reperfusion time points ($\sim 1.2\%$ increase, $P < 0.05$, Fig. 2). Treatment with MK-801 or $[Ca^{2+}]_i$ -free buffer rescued these $[Ca^{2+}]_i$ -elevating effects of NMDA under I/R conditions ($P < 0.05$, Fig. 2).

FIGURE 2. NMDAR Activity under I/R conditions drives myocardial calcium influx, effect of 30-min ischemia followed by reperfusion on isolated cardiomyocyte intracellular calcium levels ($[Ca^{2+}]_i$). Treatment with NMDA under control conditions had no significant effect on $[Ca^{2+}]_i$ relative to control. After global myocardial I/R, there was a significant increase in $[Ca^{2+}]_i$ relative to control. Treatment with NMDA under I/R conditions produced a small but significant increase in $[Ca^{2+}]_i$ at the 20-, 30-, 40-, and 50-minute reperfusion time points. Treatment with MK-801 or $[Ca^{2+}]$ -free buffer rescued the NMDA-induced elevations in $[Ca^{2+}]_i$. * $P < 0.05$ vs. control group, † $P < 0.05$ vs. I/R group.



We next assessed the cardiac performance through the analysis of left ventricular pressure signals. NMDA treatment under control conditions had no significant effect on

ventricular pressure readings ($P > 0.05$, Fig. 3). After global myocardial I/R, there were significant reductions in LVDP (~41% decrease, $P < 0.05$, Fig. 3A), $+dp/dt_{max}$ (~40%

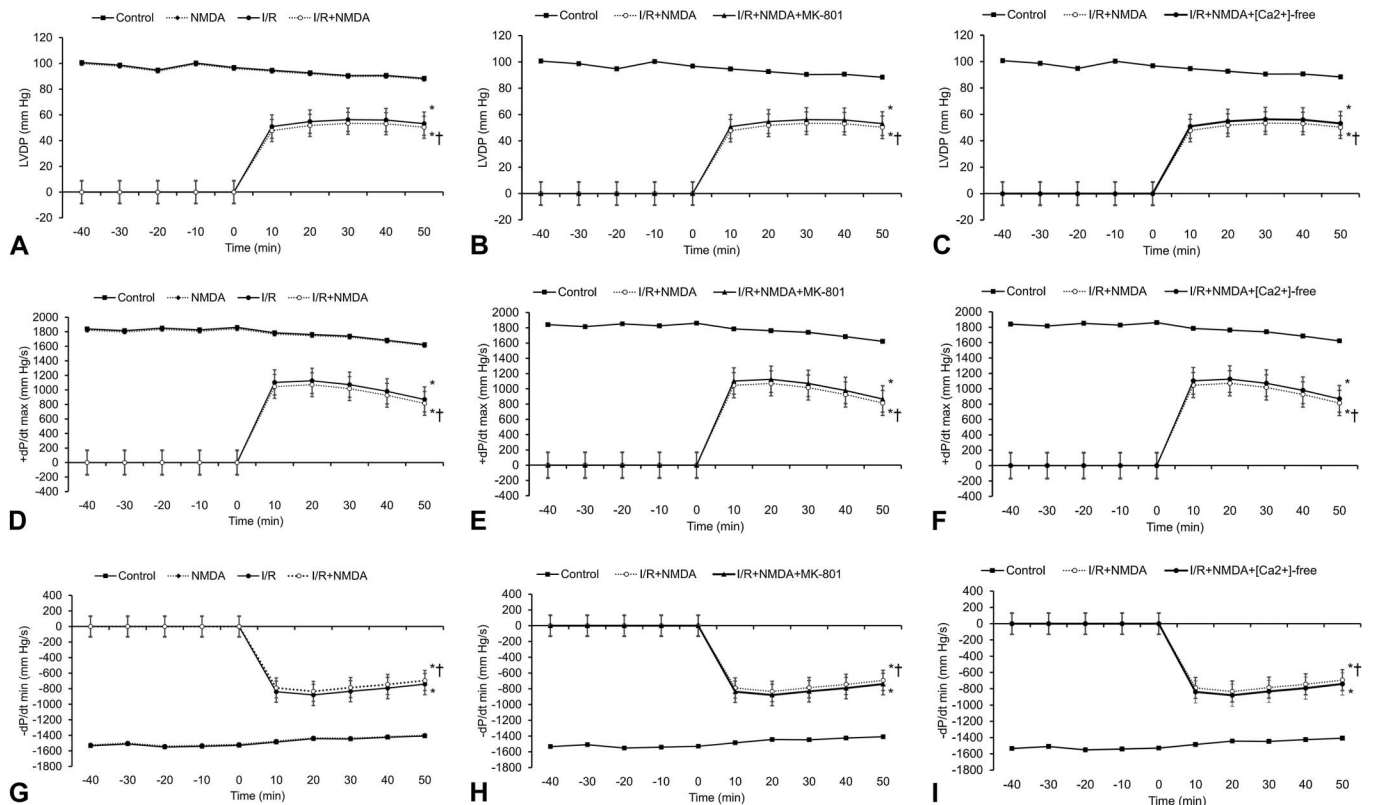
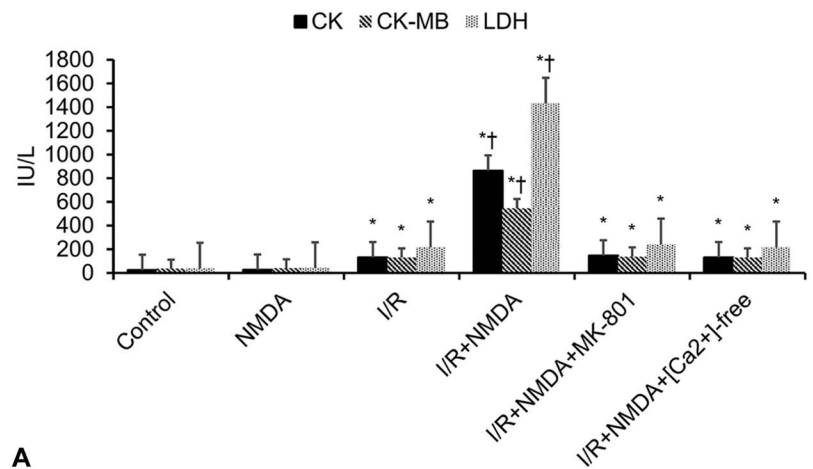


FIGURE 3. NMDAR-driven calcium influx decreases cardiac performance, Left ventricular pressure signals were recorded using the Langendorff system. Treatment with NMDA under control conditions had no significant effect on (A) LVDP, (D) $+dp/dt_{max}$, and (G) $-dp/dt_{min}$ relative to control. After global myocardial I/R, there were significant reductions in (A) LVDP, (D) $+dp/dt_{max}$, and (G) $-dp/dt_{min}$ relative to control. Treatment with NMDA under I/R conditions produced more significant reductions in (A) LVDP, (D) $+dp/dt_{max}$, and (G) $-dp/dt_{min}$. Treatment with MK-801 rescued the NMDA-induced reductions in (B) LVDP, (E) $+dp/dt_{max}$, and (H) $-dp/dt_{min}$. Treatment with $[Ca^{2+}]$ -free buffer also rescued the NMDA-induced reductions in (C) LVDP, (F) $+dp/dt_{max}$, and (I) $-dp/dt_{min}$. * $P < 0.05$ vs. control group, † $P < 0.05$ vs. I/R group.

decrease, $P < 0.05$, Fig. 3B), and $-dp/dt_{min}$ ($\sim 43\%$ decrease, $P < 0.05$, Fig. 3C), relative to control conditions. Notably, treatment with NMDA under I/R conditions produced more significant reductions in LVDP (additional $\sim 5.4\%$ decrease, $P < 0.05$, Fig. 3A), $+dp/dt_{max}$ (additional $\sim 5.4\%$ decrease, $P < 0.05$, Fig. 3B), and $-dp/dt_{min}$ (additional $\sim 5.8\%$ decrease, $P < 0.05$, Fig. 3C). Treatment with MK-801 or $[Ca^{2+}]$ -free buffer rescued these damaging effects of NMDA under I/R conditions (all $P < 0.05$, Fig. 3).

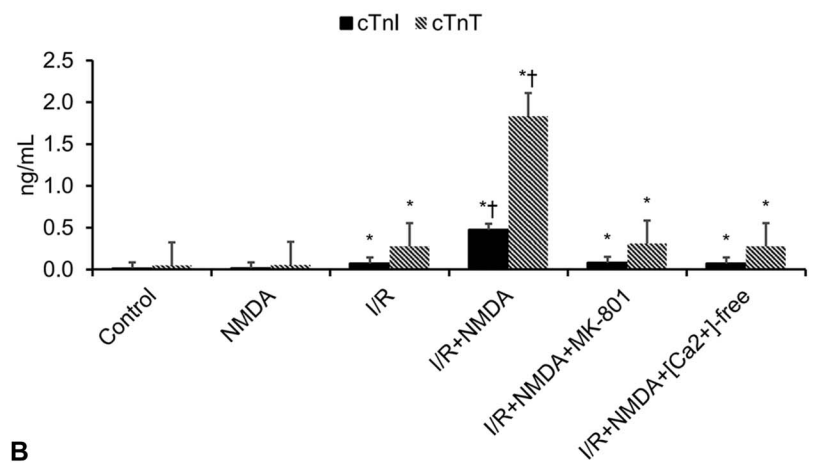
Next, we assessed the coronary effluent activity of 5 key cardiac markers (ie, CK, CK-MB, LDH, cTnI, and cTnT) to examine the extent of myocardial damage. NMDA treatment under control conditions had no significant effect on the 5 key cardiac markers ($P > 0.05$, Fig. 4). After global myocardial I/R, there were significant multi-fold increases in CK ($P < 0.05$, Fig. 4A), CK-MB ($P < 0.05$, Fig. 4A), LDH ($P < 0.05$, Fig. 4A), cTnI ($P < 0.05$, Fig. 4B), and cTnT ($P < 0.05$, Fig. 4B), relative to control conditions. Notably, treatment with NMDA under I/R conditions produced more significant multi-fold increases in all 5 cardiac markers (all $P < 0.05$, Fig. 4). Treatment with MK-801 or $[Ca^{2+}]$ -free buffer rescued the elevated levels of all 5 cardiac markers ($P < 0.05$, Fig. 4).

Isolated rat hearts initially display myocardial apoptosis after 10 minutes of ischemia and achieve a maximal level of myocardial apoptosis after 30 minutes of ischemia.¹⁸ Accordingly, the global myocardial I/R model applied here (ie, a 30-min period of global myocardial ischemia followed by a reperfusion period) has been shown to reliably produce generalized myocardial necrosis in isolated rat hearts.^{15,19–21} Using this ex vivo model, we assessed the degree of generalized myocardial necrosis and cardiomyocyte apoptosis by the TTC-based staining (Fig. 5A) and TUNEL-based staining, respectively. NMDA treatment under control conditions had no significant effect on generalized myocardial necrosis ($P > 0.05$, Fig. 5B) or cardiomyocyte apoptosis ($P > 0.05$, Fig. 5C). After global myocardial I/R, there was a significant multi-fold increase in generalized myocardial necrosis ($P < 0.05$, Fig. 5B) as well as a significant increase in cardiomyocyte apoptosis levels relative to control conditions ($\sim 130\%$ increase, $P < 0.05$, Fig. 5C). Notably, treatment with NMDA under I/R conditions produced more significant increases in generalized myocardial necrosis ($\sim 36\%$ increase, $P < 0.05$, Fig. 5B) and cardiomyocyte apoptosis ($\sim 150\%$ increase, $P < 0.05$, Fig. 5C). Treatment with MK-801 or $[Ca^{2+}]$ -free buffer rescued these damaging effects of NMDA under I/R conditions (both $P < 0.05$, Fig. 5B, C).



A

FIGURE 4. NMDAR-driven calcium influx elevates markers of myocardial damage, the activity of 5 key cardiac markers—CK, CK-MB, LDH, cTnI, and cTnT—in the coronary effluent were assessed to examine the extent of myocardial damage. Treatment with NMDA under control conditions had no significant effect on (A) CK, CK-MB, and LDH as well as (B) cTnI and cTnT relative to control. After global myocardial I/R, there were significant increases in (A) CK, CK-MB, and LDH as well as (B) cTnI and cTnT relative to control. Notably, treatment with NMDA under I/R conditions produced more significant increases in (A) CK, CK-MB, and LDH as well as (B) cTnI and cTnT. Treatment with MK-801 or $[Ca^{2+}]$ -free buffer rescued the NMDA-induced elevations in (A) CK, CK-MB, and LDH as well as (B) cTnI and cTnT. * $P < 0.05$ vs. control group, † $P < 0.05$ vs. I/R group.



B

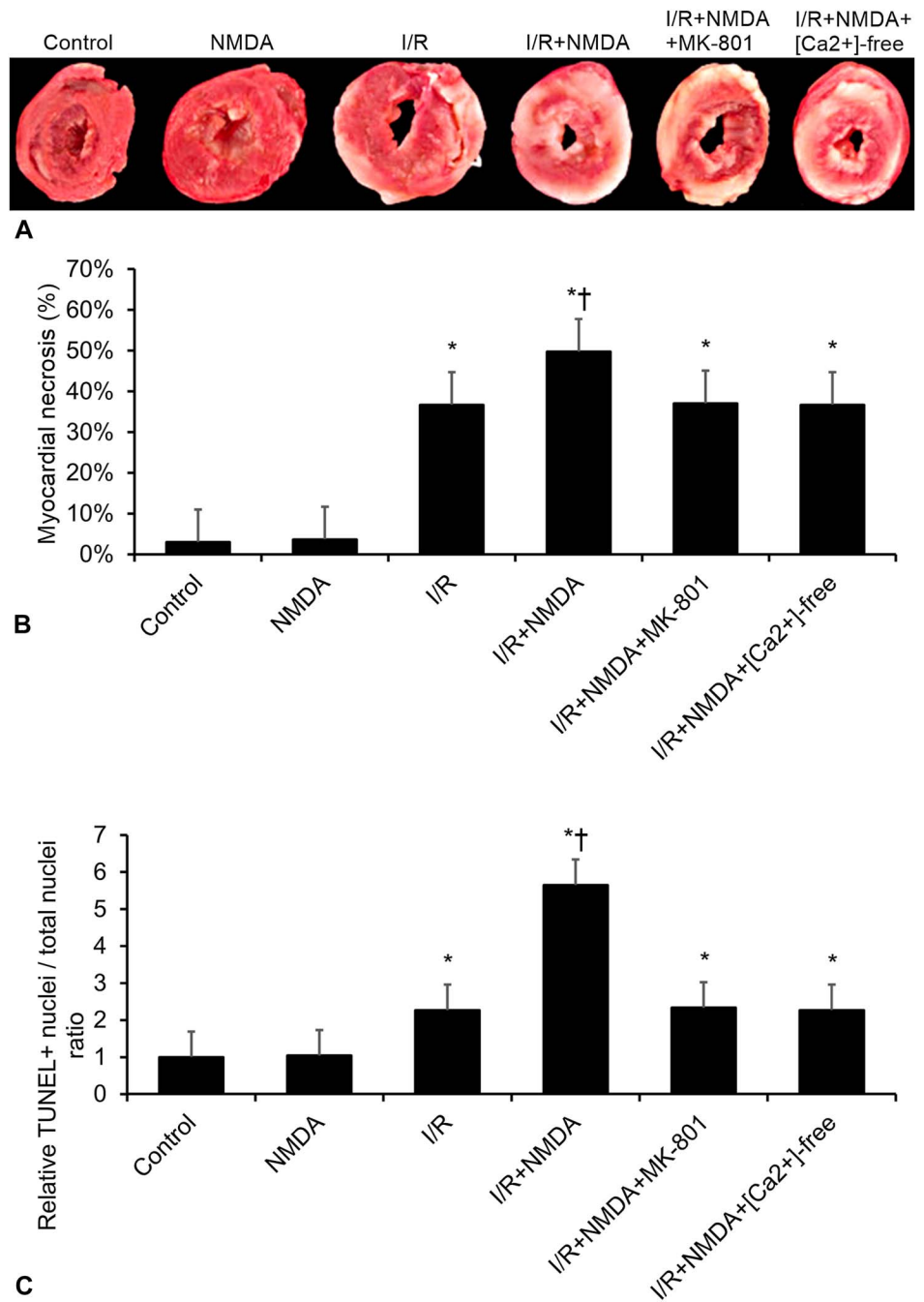


FIGURE 5. NMDAR-driven calcium influx increases generalized myocardial necrosis and apoptosis levels, TTC-based and TUNEL-based staining were applied to assess the degree of generalized myocardial necrosis and cardiomyocyte apoptosis, respectively. A, Representative images of TTC-stained rat heart cross-sections showing widely distributed necrotic areas in global myocardial I/R hearts but negligible necrosis in non-I/R hearts. Treatment with NMDA under control conditions had no significant effect on (B) generalized myocardial necrosis and (C) cardiomyocyte apoptosis relative to control. After global myocardial I/R, there was a significant increase in (B) generalized myocardial necrosis and (C) cardiomyocyte apoptosis relative to control. Treatment with NMDA produced more significant increases in (B) generalized myocardial necrosis and (C) cardiomyocyte apoptosis. Treatment with MK-801 or [Ca²⁺]-free buffer rescued the NMDA-induced increases in (B) generalized myocardial necrosis and (C) cardiomyocyte apoptosis. **P* < 0.05 vs. control group, †*P* < 0.05 vs. I/R group.

Finally, we applied Western blotting to assess the phosphorylation of 4 protein kinases that have been previously associated with myocardial ischemia and ischemic cardioprotection (ie, PKC-δ, PKC-ε, Akt, and ERK).²²⁻²⁴ NMDA treatment under control conditions had no significant effect on the activation of the 4 protein kinases (all *P* > 0.05, Fig. 6). After global myocardial I/R, there were significant increases in the phosphorylation of PKC-δ (*P* < 0.05, Fig. 6A), PKC-ε (*P* < 0.05, Fig. 6B), Akt(Ser⁴⁷³) and Akt(Thr³⁰⁸) (both *P* < 0.05, Fig. 6C), and ERK (*P* < 0.05, Fig. 6D) relative to control conditions. Notably, treatment

with NMDA under I/R conditions produced more significant multi-fold increases in the phosphorylation of all 4 protein kinases (all *P* < 0.05, Fig. 6). Treatment with MK-801 or [Ca²⁺]-free buffer rescued the elevated phosphorylation levels of all 4 protein kinases (all *P* < 0.05, Fig. 6).

DISCUSSION

The objective of this study was to comprehensively evaluate the effects of NMDAR activity through an ex vivo global myocardial I/R rat model. We found that enhanced

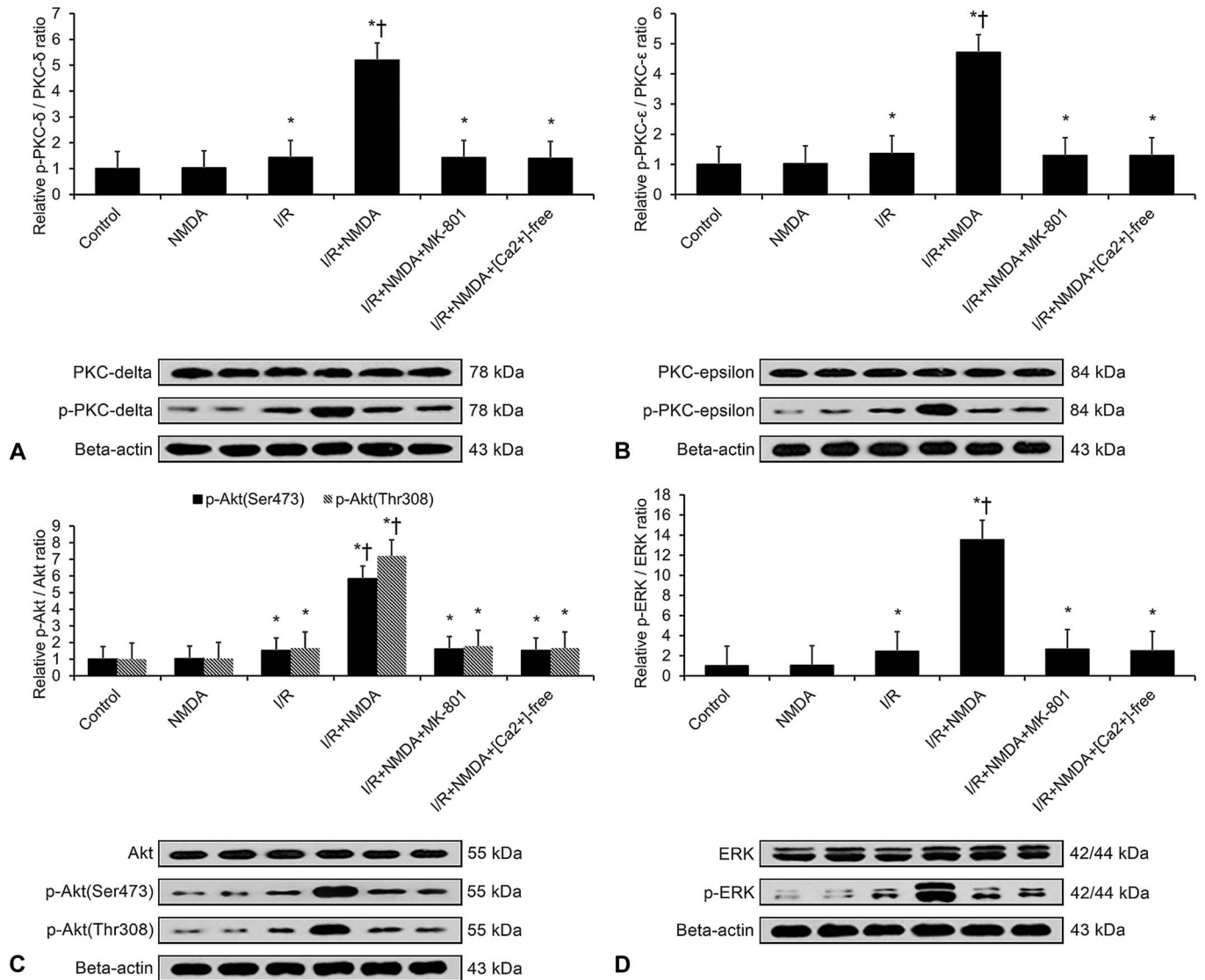


FIGURE 6. NMDAR-driven calcium influx elevates protein kinase expression, Western blotting to assess the phosphorylation of 4 protein kinases: PKC- δ , PKC- ϵ , Akt, and ERK. Treatment with NMDA under control conditions had no significant effect on the phosphorylation of (A) PKC- δ , (B) PKC- ϵ , (C) Akt(Ser⁴⁷³) and Akt(Thr³⁰⁸), and (D) ERK relative to control. After global myocardial I/R, there were significant increases in the phosphorylation of (A) PKC- δ , (B) PKC- ϵ , (C) Akt(Ser⁴⁷³) and Akt(Thr³⁰⁸), and (D) ERK relative to control. Notably, treatment with NMDA produced more significant increases in the phosphorylation of (A) PKC- δ , (B) PKC- ϵ , (C) Akt(Ser⁴⁷³) and Akt(Thr³⁰⁸), and (D) ERK. Treatment with MK-801 or [Ca²⁺]_i-free buffer rescued the NMDA-induced increases in the phosphorylation of (A) PKC- δ , (B) PKC- ϵ , (C) Akt(Ser⁴⁷³) and Akt(Thr³⁰⁸), and (D) ERK. **P* < 0.05 vs. control group, †*P* < 0.05 vs. I/R group.

NMDAR activity (through NMDA treatment) under I/R conditions produces significant increases in [Ca²⁺]_i levels, significant losses in left ventricular function, significant increases in markers of myocardial damage, significant increases in generalized myocardial necrosis and cardiomyocyte apoptosis, and significant increases in the phosphorylation of PKC- δ , PKC- ϵ , Akt, and ERK. These adverse effects were rescued by either treatment with the NMDAR inhibitor MK-801 or [Ca²⁺]_i-free buffer. In contrast, enhanced NMDAR activity under control conditions had no significant effects on the foregoing variables. These combined findings

indicate that NMDAR-driven calcium influx potentiates the adverse effects of myocardial I/R injury ex vivo.

Our findings show that NMDAR activity under I/R conditions promotes myocardial calcium influx. Consistent with our findings, previous studies on rodent I/R heart models have demonstrated that a 30-minute period of global myocardial ischemia followed by a reperfusion period results in significant increases in [Ca²⁺]_i.^{25,26} Interestingly, these same studies also demonstrate no significant changes in [Ca²⁺]_i levels for ischemic periods under 30 minutes in duration.^{25,26} As ischemic damage in murine and rodent hearts is fully

reversible on reperfusion after ischemic periods of less than 30 minutes, Saini et al has postulated that the increased $[Ca^{2+}]_i$ levels found in I/R heart models after 30 minutes of ischemia may be exclusively linked to conditions of irreversible myocardial ischemic injury.¹⁶ On this basis, our current findings suggest that NMDAR activity potentiates myocardial calcium influx solely under conditions of irreversible myocardial ischemic injury. Further studies on NMDAR activity involving myocardial ischemic periods of less than 30 minutes are needed to verify this hypothesis.

Our findings show that NMDAR-driven calcium influx adversely affects myocardial performance under I/R conditions, as demonstrated by (1) the significant increase in $[Ca^{2+}]_i$ levels coupled with (2) the significant LVDP reduction in NMDA-treated hearts under I/R conditions, both of which were rescued by treatment with MK-801 or $[Ca^{2+}]$ -free buffer. Moreover, our data revealed that this NMDAR-driven calcium influx under I/R conditions results in a less significant $-dP/dt_{min}$ during I/R. As $-dP/dt$ correlates with sarcoplasmic reticulum calcium re-uptake, NMDAR-driven calcium influx likely promotes SR calcium-ATPase activity as well as slower ventricular relaxation under I/R conditions.²⁷ Thus, according to the Frank–Starling relationship, NMDAR-driven calcium influx under I/R conditions may also result in a less significant end-diastolic volume as well as lessened ventricular force production.²⁷ Notably, NMDAR activation under control conditions had no significant effect on LVDP, $+dp/dt_{max}$, or $-dp/dt_{min}$. This concurs with previous findings by Shi et al in adult rats, who showed that chronic intraperitoneal NMDA therapy ($3 \text{ mg} \cdot \text{ml}^{-1} \cdot \text{kg}^{-1}$) produces no significant effects on key cardiac function parameters (ie, fractional shortening, left ventricular end-diastolic and end-systolic dimensions, left ventricular ejection fraction).²⁸ As extracellular levels of the NMDA agonists, glutamate and aspartate, have been shown to rise in the myocardium during I/R,^{29,30} our current findings suggest that the presence of I/R-induced NMDAR stimulants other than NMDA may be necessary to drive the NMDAR-gated $[Ca^{2+}]$ overload required to significantly disrupt cardiac function.³¹

Our findings also show that NMDAR-driven calcium influx adversely affects myocardial survival under I/R conditions, as demonstrated by the significant increases in myocardial damage markers, generalized myocardial necrosis, and apoptosis levels in NMDA-treated hearts that was rescued by treatment with MK-801 or $[Ca^{2+}]$ -free buffer. Consistent with the present findings, previous *in vivo* CNS research has shown that blocking NMDAR activity or disrupting downstream NMDAR signaling activity results in reduced postischemic cerebral infarct size.^{32–34} This NMDAR-driven cerebral damage has been attributed to the calcium influx by pannexin hemichannels and TRPV7 channels.^{35,36} Therefore, although this is the first study to demonstrate that NMDAR-driven calcium influx potentiates the adverse effects of myocardial I/R injury *ex vivo*, it is possible that NMDAR activity also promotes the activation of other calcium channels that may contribute to the observed effects. For instance, previous research in OGD cardiomyocytes suggests that hemichannel-based calcium influx occurs during the first hour of ischemia, whereas other types of

calcium influx (eg, L/T-type channels, sodium/calcium exchangers, and intracellular release channels) seem to dominate during the second hour of ischemia.³⁷ Future research should examine NMDAR's effects on the range of myocardial calcium channel types to further investigate this issue.

To examine downstream protein kinase activity associated with NMDAR-driven calcium influx, we assessed the phosphorylation levels of 4 protein kinases, which have been previously linked to myocardial ischemia and ischemic cardioprotection: PKC- δ , PKC- ϵ , Akt, and ERK.^{22–24} PKC family isoforms act as downstream signal transduction intermediaries of phospholipase C/D-driven diacylglycerol signaling.³⁸ In particular, the PKC- δ and PKC- ϵ isoforms have been associated with myocardial I/R.^{39–42} Specifically, PKC- δ and PKC- ϵ have been shown to activate and translocate in both cultured cardiomyocytes and isolated rat hearts under brief I/R conditions.^{23,41} Here, we found that NMDAR-driven calcium influx increased PKC- δ and PKC- ϵ phosphorylation levels under I/R conditions, indicating that NMDAR-driven calcium influx potentiates the PKC- δ/ϵ -activating effects of myocardial I/R. However, as PKC- δ and PKC- ϵ phosphorylation are DAG-dependent and are not calcium dependent,⁴³ the increased levels of PKC- δ and PKC- ϵ phosphorylation seen here cannot be directly attributed to NMDAR-driven calcium influx but may result from increased phospholipase C/D-driven DAG synthesis from calcium influx-induced ROS generation.⁴⁴

Akt is a cardioprotective protein kinase, which is activated under I/R conditions, where it serves to block cardiomyocyte apoptosis.^{45,46} For instance, gains in Akt (Ser⁴⁷³) and Akt(Thr³⁰⁸) phosphorylation have been positively linked with myocardial I/R in *ex vivo* isolated heart models.^{47–50} Here, NMDAR-driven calcium influx enhanced Akt(Ser⁴⁷³) and Akt(Thr³⁰⁸) phosphorylation under I/R conditions, indicating that NMDAR-driven calcium influx potentiates the Akt-activating effects of myocardial I/R. As Akt activation provides a cardioprotective effect under I/R conditions;^{45,46} the increased Akt phosphorylation observed in NMDA-treated hearts here may reveal an Akt-based protective feedback mechanism against the pro-apoptotic effects of NMDAR-driven calcium influx.

Similar to Akt, ERK is also a cardioprotective protein kinase, which is activated under I/R conditions.⁵¹ Specifically, previous findings in cultured cardiomyocytes and isolated rat hearts under I/R conditions have shown that ERK activation promotes cardiomyocyte survival by counteracting JNK and p38-induced apoptosis.⁵¹ As ERK activation provides a protective effect against cardiomyocyte apoptosis under I/R conditions,⁵¹ the increased ERK phosphorylation observed in NMDA-treated hearts here may represent a protective feedback mechanism against the pro-apoptotic effects of NMDAR-driven calcium influx.

There are several limitations to this study. First, this study's findings were limited to an *ex vivo* isolated rat heart model. Thus, our findings may not be directly translatable to *in vivo* myocardial I/R injury in humans. Second, we did not assess whether the rescue effect of inhibiting NMDAR by MK-801 would be as effective if applied during I/R as opposed to before I/R. Third, although we demonstrated that

NMDAR-driven calcium influx promotes PKC- δ , PKC- ϵ , Akt, and ERK phosphorylation under I/R conditions, it is possible that other signaling effectors are influenced by NMDAR-induced calcium influx as well. Thus, future research should investigate changes in other signaling pathways related to myocardial I/R injury, such as p38 mitogen-activated protein kinase, JNK, Src, and Lck (23). Fourth, NMDAR knockdown and overexpression experiments were not conducted here. Thus, future investigations should apply these molecular techniques to validate our conclusions.

In conclusion, NMDAR-driven calcium influx under I/R conditions produces significant increases in $[Ca^{2+}]_i$ levels, significant losses in left ventricular function, significant increases in markers of myocardial damage, significant increases in generalized myocardial necrosis and cardiomyocyte apoptosis, and significant increases in the phosphorylation of PKC- δ , PKC- ϵ , Akt, and ERK. As NMDAR-driven calcium influx adversely influences cardiac performance and myocardial survival under I/R conditions, these findings suggest that NMDAR antagonism may be an effective ancillary therapeutic strategy for myocardial I/R injury.

REFERENCES

- Sanz-Clemente A, Nicoll RA, Roche KW. Diversity in NMDA receptor composition many regulators, many consequences. *Neuroscientist*. 2013;19:62–75.
- Gilmour G, Dix S, Fellini L, et al. NMDA receptors, cognition and schizophrenia—testing the validity of the NMDA receptor hypofunction hypothesis. *Neuropharmacology*. 2012;62:1401–1412.
- Schwartz BL, Hashtroudi S, Herting RL, et al. The NMDA receptor complex: enhancement of memory in aging and dementia. *Basic Appl Mem Res*. 2013;2:423–437.
- Takahashi H, Xia P, Cui J, et al. Pharmacologically targeted NMDA receptor antagonism by NitroMemantine for cerebrovascular disease. *Sci Rep*. 2015;6:20750.
- Sun Y, Zhang L, Chen Y, et al. Therapeutic targets for cerebral ischemia based on the signaling pathways of the GluN2B C terminus. *Stroke*. 2015;46:2347–2353.
- Parsons MP, Raymond LA. Extrasynaptic NMDA receptor involvement in central nervous system disorders. *Neuron*. 2014;82:279–293.
- Grupke S, Hall J, Dobbs M, et al. Understanding history, and not repeating it. Neuroprotection for acute ischemic stroke: from review to preview. *Clin Neurol Neurosurg*. 2015;129:1–9.
- Gill SS, Pulido OM, Mueller RW, et al. Molecular and immunochemical characterization of the ionotropic glutamate receptors in the rat heart. *Brain Res Bull*. 1998;46:429–434.
- Gill SS, Pulido OM, Mueller RW, et al. Immunochemical localization of the metabotropic glutamate receptors in the rat heart. *Brain Res Bull*. 1999;48:143–146.
- Tauskela JS, Murray CL, Wang Y, et al. Evidence from cultured rat cortical neurons of differences in the mechanism of ischemic preconditioning of brain and heart. *Brain Res*. 1999;827:143–151.
- Gao X, Xu X, Pang J, et al. NMDA receptor activation induces mitochondrial dysfunction, oxidative stress and apoptosis in cultured neonatal rat cardiomyocytes. *Physiol Res*. 2007;56:559.
- Skeberdis VA, Lan J-Y, Opitz T, et al. mGluR1-mediated potentiation of NMDA receptors involves a rise in intracellular calcium and activation of protein kinase C. *Neuropharmacology*. 2001;40:856–865.
- Krapivinsky G, Krapivinsky L, Manasian Y, et al. The NMDA receptor is coupled to the ERK pathway by a direct interaction between NR2B and RasGRF1. *Neuron*. 2003;40:775–784.
- Care IoLARCo, Animals UoL, Resources NIoHDoR. *Guide for the Care and Use of Laboratory Animals*. Washington, DC: National Academies; 1985.
- Hu J, Li Z, Xu L-T, et al. Protective effect of apigenin on ischemia/reperfusion injury of the isolated rat heart. *Cardiovasc Toxicol*. 2015;15:241–249.
- Saini HK, Dhalla NS. Defective calcium handling in cardiomyocytes isolated from hearts subjected to ischemia-reperfusion. *Am J Physiol Heart Circ Physiol*. 2005;288:H2260–H2270.
- Gryniewicz G, Poenie M, Tsien RY. A new generation of Ca^{2+} indicators with greatly improved fluorescence properties. *J Biol Chem*. 1985;260:3440–3450.
- Chakrabarti S, Hoque AE, Karmazyn M. A rapid ischemia-induced apoptosis in isolated rat hearts and its attenuation by the sodium–hydrogen exchange inhibitor HOE 642 (cariporide). *J Mol Cell Cardiol*. 1997;29:3169–3174.
- Okamura T, Miura T, Takemura G, et al. Effect of caspase inhibitors on myocardial infarct size and myocyte DNA fragmentation in the ischemia–reperfused rat heart. *Cardiovasc Res*. 2000;45:642–650.
- Penna C, Cappello S, Mancardi D, et al. Post-conditioning reduces infarct size in the isolated rat heart: role of coronary flow and pressure and the nitric oxide/cGMP pathway. *Basic Res Cardiol*. 2006;101:168–179.
- Hayashida K, Sano M, Ohsawa I, et al. Inhalation of hydrogen gas reduces infarct size in the rat model of myocardial ischemia–reperfusion injury. *Biochem biophysical Res Commun*. 2008;373:30–35.
- Alloaati G, Arnoletti E, Bassino E, et al. Obestatin affords cardioprotection to the ischemic-reperfused isolated rat heart and inhibits apoptosis in cultures of similarly stressed cardiomyocytes. *Am J Physiol Heart Circ Physiol*. 2010;299:H470–H481.
- Kawamura S, Yoshida K-I, Miura T, et al. Ischemic preconditioning translocates PKC- δ and - ϵ , which mediate functional protection in isolated rat heart. *Am J Physiol Heart Circ Physiol*. 1998;275:H2266–H2271.
- Armstrong SC. Protein kinase activation and myocardial ischemia/reperfusion injury. *Cardiovasc Res*. 2004;61:427–436.
- Meissner A, Morgan JP. Contractile dysfunction and abnormal Ca^{2+} modulation during postischemic reperfusion in rat heart. *Am J Physiol Heart Circ Physiol*. 1995;268:H100–H111.
- Seki S, Horikoshi K, Takeda H, et al. Effects of sustained low-flow ischemia and reperfusion on Ca^{2+} transients and contractility in perfused rat hearts. *Mol Cell Biochem*. 2001;216:111–119.
- Demirel HA, Powers SK, Zergeroglu MA, et al. Short-term exercise improves myocardial tolerance to in vivo ischemia-reperfusion in the rat. *J Appl Physiol*. 2001;91:2205–2212.
- Shi S, Liu T, Li Y, et al. Chronic N-Methyl-D-Aspartate receptor activation induces cardiac electrical remodeling and increases susceptibility to ventricular arrhythmias. *Pacing Clin Electrophysiol*. 2014;37:1367–1377.
- Liu Z, Vuohelainen V, Tarkka M, et al. Glutamate release predicts ongoing myocardial ischemia of rat hearts. *Scand J Clin Lab Invest*. 2010;70:217–224.
- Bäckström T, Gojny M, Lockowandt U, et al. Cardiac outflow of amino acids and purines during myocardial ischemia and reperfusion. *J Appl Physiol*. 2003;94:1122–1128.
- Sun X, Zhong J, Wang D, et al. Increasing glutamate promotes ischemia-reperfusion-induced ventricular arrhythmias in rats in vivo. *Pharmacology*. 2013;93:4–9.
- Gotti B, Duverger D, Bertin J, et al. Ifenprodil and SL 82.0715 as cerebral anti-ischemic agents. I. Evidence for efficacy in models of focal cerebral ischemia. *J Pharmacol Exp Ther*. 1988;247:1211–1221.
- Tu W, Xu X, Peng L, et al. DAPK1 interaction with NMDA receptor NR2B subunits mediates brain damage in stroke. *Cell*. 2010;140:222–234.
- Aarts M, Liu Y, Liu L, et al. Treatment of ischemic brain damage by perturbing NMDA receptor-PSD-95 protein interactions. *Science*. 2002;298:846–850.
- Weilinger NL, Tang PL, Thompson RJ. Anoxia-induced NMDA receptor activation opens pannexin channels via Src family kinases. *J Neurosci*. 2012;32:12579–12588.
- Aarts M, Iihara K, Wei W-L, et al. A key role for TRPM7 channels in anoxic neuronal death. *Cell*. 2003;115:863–877.
- Shintani-Ishida K, Uemura K, Yoshida K. Hemichannels in cardiomyocytes open transiently during ischemia and contribute to reperfusion injury following brief ischemia. *Am J Physiol Heart Circ Physiol*. 2007;293:H1714–H1720.

38. Song M, Matkovich SJ, Zhang Y, et al. Combined cardiomyocyte PKC δ and PKC ϵ gene deletion uncovers their central role in restraining developmental and reactive heart growth. *Sci Signal*. 2015;8:39.
39. Churchill EN, Murriel CL, Chen C-H, et al. Reperfusion-induced translocation of δ PKC to cardiac mitochondria prevents pyruvate dehydrogenase reactivation. *Circ Res*. 2005;97:78–85.
40. Murriel CL, Churchill E, Inagaki K, et al. Protein kinase C δ activation induces apoptosis in response to cardiac ischemia and reperfusion damage a mechanism involving bad and the mitochondria. *J Biol Chem*. 2004;279:47985–47991.
41. Mitchell MB, Meng X, Ao L, et al. Preconditioning of isolated rat heart is mediated by protein kinase C. *Circ Res*. 1995;76:73–81.
42. Ping P, Zhang J, Qiu Y, et al. Ischemic preconditioning induces selective translocation of protein kinase C isoforms ϵ and η in the heart of conscious rabbits without subcellular redistribution of total protein kinase C activity. *Circ Res*. 1997;81:404–414.
43. Zheng H, Liu J, Liu C, et al. Calcium-sensing receptor activating phosphorylation of PKC δ translocation on mitochondria to induce cardiomyocyte apoptosis during ischemia/reperfusion. *Mol Cell Biochem*. 2011;358:335–343.
44. Inagaki K, Churchill E, Mochly-Rosen D. Epsilon protein kinase C as a potential therapeutic target for the ischemic heart. *Cardiovasc Res*. 2006;70:222–230.
45. Fujio Y, Nguyen T, Wencker D, et al. Akt promotes survival of cardiomyocytes in vitro and protects against ischemia-reperfusion injury in mouse heart. *Circulation*. 2000;101:660–667.
46. Miao W, Luo Z, Kitsis RN, et al. Intracoronary, adenovirus-mediated Akt gene transfer in heart limits infarct size following ischemia-reperfusion injury in vivo. *J Mol Cell Cardiol*. 2000;32:2397–2402.
47. Hiroyuki O, Noritoshi N, Takefumi I. Adrenomedullin infusion attenuates myocardial ischemia/reperfusion injury through the phosphatidylinositol 3-kinase/Akt-dependent pathway. *Circulation*. 2004;109:242–248.
48. Ha T, Hua F, Liu X, et al. Lipopolysaccharide-induced myocardial protection against ischemia/reperfusion injury is mediated through a PI3K/Akt-dependent mechanism. *Cardiovasc Res*. 2008;78:546–553.
49. Keyes KT, Ye Y, Lin Y, et al. Resolvin E1 protects the rat heart against reperfusion injury. *Am J Physiol Heart Circ Physiol*. 2010;299:H153–H64.
50. Ma H, Guo R, Yu L, et al. Aldehyde dehydrogenase 2 (ALDH2) rescues myocardial ischaemia/reperfusion injury: role of autophagy paradox and toxic aldehyde. *Eur Heart J*. 2011;32:1025–1038.
51. Yue T-L, Wang C, Gu J-L, et al. Inhibition of extracellular signal-regulated kinase enhances ischemia/reoxygenation-induced apoptosis in cultured cardiac myocytes and exaggerates reperfusion injury in isolated perfused heart. *Circ Res*. 2000;86:692–699.